Journal of ELECTRONIC MATERIALS, Vol. 35, No. 11, 2006 *Regular Issue Paper*

Model of Shear Viscosity for Underfill Flows

R. YANG,[1] D.C. SUN,[2,3] and SEUNGBAE PARK[2]

1.—Spirent Communications, Inc., 15200 Omega Drive, Rockville, MD 20850. 2.—Department of Mechanical Engineering, State University of New York at Binghamton, Binghamton, NY 13902–6000. 3.—E-mail: dcsun@binghamton.edu

To analyze the flow of an underfill encapsulant between the chip and substrate, a shear viscosity model is needed. This paper presents a model of the viscosity for the flow of slurry between two parallel walls, which is a typical situation found in electronic packaging applications. It is postulated that the flow behavior of a dense slurry is governed by the particle-particle and particle-wall interactions. Fluid film lubrication theory is used to find the unit solutions of interaction between two particles. The unit solutions are applied to the simple case of slurry flow densely packed with neutrally buoyant particles. The dependence of the effective viscosity of the slurry on packing parameters is revealed.

Key words: Underfill encapsulant, underfill flow, effective viscosity, neutrally buoyant

INTRODUCTION

Encapsulation is an integral part of electronic packaging especially in flip-chip packages and chip-on-board (COB) applications. The purpose of encapsulation is to protect the solder interconnects linking the silicon chip and the substrate from damages arising from the mismatch of the coefficients of thermal expansion (CTE) of the two materials. The encapsulant is a thermosetting epoxy filled with particles (or fillers) in high volume fraction. Flow of the encapsulant into the gap between the chip and the substrate, called the underfill flow, is driven by capillary action governed by the small height of the gap. Two manufacturing concerns arise regarding the underfill flow. One is the slow flow speed that makes the filling process inefficient. The other is formation of voids around the solder interconnects that reduces the reliability of the package. To improve on these aspects, the underfill flow process needs to be better understood.

Since the pioneering work of Washburn,[1] capillary flows have been analyzed by considering the flow to consist of two regions: the marching front region and the bulk flow region following the marching front. In the marching front region, surface tension draws the meniscus to move forward and induces a pressure drop behind the meniscus. The liquid in the bulk region is considered to be driven by the pressure difference between the low pressure at the front caused by surface tension and the higher ambient pressure behind the liquid. However, the two regions of flow are coupled. The bulk flow velocity determines the marching velocity of the meniscus, which is related to the contact angle(s) between the liquid and the solid boundaries. The contact angle(s), in turn, affects the pressure drop behind the meniscus. Therefore, a complete treatment of capillary flows involves the interaction between the two regions of flow. In the bulk flow region, the most important material parameter is the viscosity of the liquid.

Using Washburn's approach, underfill encapsulant flows have also been analyzed.[2,3] However, the fluid in this study is a dense slurry consisting of a liquid carrier and filling particles in high volume fraction. A key question may thus be posed: if the slurry is modeled as a single phase fluid, then what should its effective viscosity be?

Numerous studies were made on the viscosity of a mixture. Einstein[4] obtained a formula for the effective viscosity of a dilute mixture, applicable when the volume fraction ϕ, defined as the volume of solid particles per unit volume of the mixture, is less than ~3%. Leighton and Acrivos[5] proposed a formula that extends the volume fraction range to much higher values,

$$\mu_{\text{eff}}/\mu = \left(1 + \frac{1.5\phi}{1 - \frac{\phi}{\phi_0}}\right)^2 \qquad (1)$$

where μ_{eff} is the effective viscosity, μ the liquid viscosity, and ϕ_0 the volume fraction at the closest

(Received February 22, 2006; accepted June 12, 2006)

packing. This formula is based on the assumptions that the particle diameter is much smaller than the channel size and that the mixture flow obeys the no-slip boundary condition at the channel walls. The flow behavior of mixtures has also been studied by numerical simulation techniques[6] using the assumptions mentioned above, and by experiments, e.g., the recent work of Prasad and Kytomaa.[7] In their work, the viscometer was designed in such a way that particles were embedded in the channel walls to simulate the no-slip boundary condition.

In the case of underfill flows, the gap between the chip and the substrate is ~70 μm or less, and the particle size is ~5–10 μm. Hence, the particle size is not much smaller than the channel size. Besides, the volume fraction in an encapsulant is approaching to that possible at the closest packing. Equation 1 then results in an effective viscosity value of infinity. In a recent work,[8] a correlation formula for the effective viscosity based on measured data was presented. That formula is essentially Eq. 1 multiplied by a factor that corrects the effect of shear rate. At the maximum volume fraction, the formula also predicts infinite viscosity. Thus, formulas similar to Eq. 1 might not be applicable for mixtures with high volume fraction fillers.

In this study, the slow motion of a dense slurry in a vertical glass tube (10 mm inner diameter) was observed. The slurry was made of glass beads (1 mm outer diameter) mixed in honey. After the glass tube was filled with the slurry, the plug at the bottom of the tube was removed to start the flow. It was observed that the glass beads next to the tube wall translated, and even slowly rotated, relative to the wall. This latter aspect was also observed in particulate two-phase flows by Acrivos.[9] In our experiment, except very near the wall, the beads translated almost as a slug, i.e., they appeared to have no relative motion with respect to each other. A slug flow model is thus envisioned wherein the flow behavior of a dense slurry may be governed by the interactions between neighboring particles and between particles and their neighboring walls through thin liquid films trapped between the solid surfaces. Because of the small clearances between the solid surfaces, it may be feasible to study the flow behavior by using fluid film lubrication theory. In this work, formulas for the interaction forces and leakage flow rates are derived based on fluid film lubrication theory for a Newtonian liquid. In the section "Slug Flow Model," these formulas are applied to the flow of a slurry containing one-size, neutrally buoyant, spherical particles. The analysis is aimed at obtaining the effective viscosity for this type of slurry flow. The situation of arbitrary shape and nonuniform size of the particles is not addressed in this analysis.

In the literature (e.g., Ref. 8) encapsulants are often modeled as viscoelastic fluids. The rheological equations used are invariably modifications of Newtonian viscosity (of the encapsulant) with factors or terms correcting for the effect of shear rate. Nevertheless, there does not appear to exist a model for the Newtonian viscosity itself in the densely packed limit. The present work is intended to provide such a model.

UNIT SOLUTIONS FOR INTERACTIONS BETWEEN TWO PARTICLES

Consider two spherical particles interacting with each other through a thin liquid film between them. If the two spheres approach each other along their center line, the liquid film is subjected to a squeeze action, and a normal resistance force (i.e., along the center line) is developed. If the two spheres rotate with respect to each other, the liquid film is subjected to entrainment action, and then both a normal separating force and friction forces tangent to the surfaces of the spheres are developed. These two types of actions are treated separately.

Squeeze Action

Figure 1a shows two spheres approaching each other and the polar coordinate system used in the analysis. Let the radii of the two spheres be R_1 and R_2. The gap between the two surfaces may be approximated by

$$h(r,t) = h_0(t) + \frac{r^2}{2R_1} + \frac{r^2}{2R_2},\ r \ll R_1 \text{ or } R_2 \qquad (2)$$

This gap function is equivalent to that between a sphere of radius R_e and a plane,

$$h(r,t) = h_0(t) + \frac{r^2}{2R_e} \qquad (3)$$

where R_e, called the reduced radius, is given as

$$\frac{1}{R_e} = \frac{1}{R_1} + \frac{1}{R_2} \qquad (4)$$

In the above, $h_0(t)$ is the liquid film thickness at the smallest gap. Because h_0/R_e is much smaller than unity, lubrication approximations may be invoked that greatly simplify analysis of the flow.

The simplified equations governing the film flow are

$$\frac{1}{r}\frac{\partial}{\partial r}(rV_r) + \frac{\partial V_z}{\partial z} = 0 \qquad (5)$$

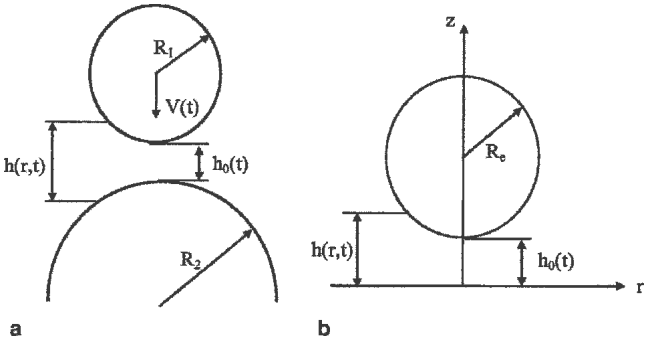

Fig. 1. Squeeze action between two spheres: (a) two rigid spheres separated by a liquid film; (b) equivalent system of a rigid sphere of effective radius R_e.

$$\frac{\partial p}{\partial z} = 0 \tag{6}$$

$$\frac{\partial p}{\partial r} = \mu \frac{\partial^2 V_r}{\partial z^2} \tag{7}$$

where V_r and V_z are the velocity components of flow in the r and z directions, respectively, p is the pressure, and μ is the viscosity of the liquid film. The boundary conditions for the velocity components are

$$\begin{aligned} &\text{At } z = 0,\ V_r = 0 \text{ and } V_z = 0 \\ &\text{At } z = h,\ V_r = 0 \text{ and } V_z = -V(t) \end{aligned} \tag{8}$$

The system above can be reduced to a single equation for the pressure:

$$\frac{\partial p}{\partial r} = -6\mu V \frac{r}{h^3} \tag{9}$$

which can be solved with the boundary condition

$$p \to 0 \text{ when } \frac{r^2}{2R_e h_0} \gg 1 \tag{10}$$

Integrating the pressure solution over the film domain, one obtains the normal separating force

$$W \approx 6\pi\mu V R_e \left(\frac{R_e}{h_0}\right) \tag{11}$$

The equation shows that the normal separating force is of the order $\frac{R_e}{h_0}$ if $h_0 \ll R_e$. When h_0 approaches R_e, the normal separating force reduces to

$$W = 6\pi\mu V R_e \tag{12}$$

which is the well-known Stokes' law of drag for a sphere translating in a viscous fluid.

Entrainment Action

When two spheres spaced h_0 apart rotate relative to each other, the surrounding liquid is entrained into the gap. As a result, a normal force is developed to separate the spheres, and friction forces are developed countering the rotational motion. Figure 2 shows a sketch of this interaction. Here, a Cartesian coordinate system is used where the (x, y) plane is normal to the line of centers and rotations are about the y axis.

The gap function between the two spheres is given by

$$h(x, y) = h_1 + h_2 \tag{13}$$

where h_1 and h_2 are approximated as

$$h_1 = \frac{h_0}{2} + \frac{x^2 + y^2}{2R_1} \tag{14}$$

$$h_2 = \frac{h_0}{2} + \frac{x^2 + y^2}{2R_2} \tag{15}$$

With the reduced radius R_e defined in Eq. 4, the gap function can be expressed as

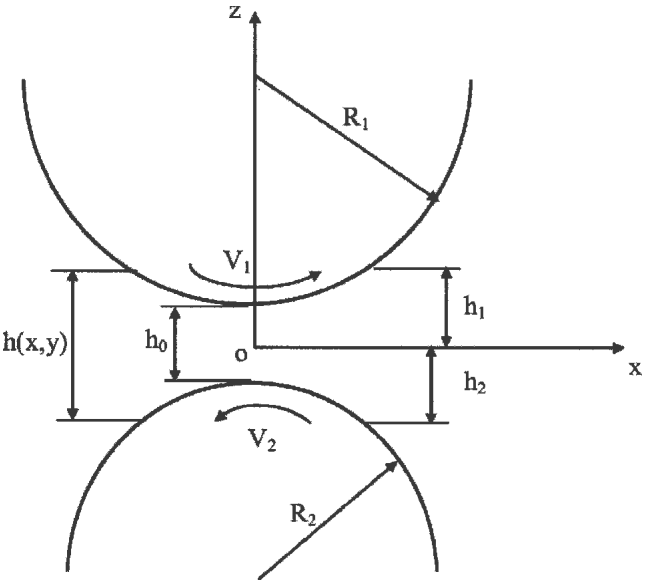

Fig. 2. Entrainment action between two rotating spheres.

$$h(x, y) = h_0 + \frac{x^2 + y^2}{2R_e} \tag{16}$$

Because h_0/R_e is much smaller than unity, lubrication approximations may be used and the governing equations take the form:

$$\frac{\partial V_x}{\partial x} + \frac{\partial V_y}{\partial y} + \frac{\partial V_z}{\partial z} = 0 \tag{17}$$

$$\partial p/\partial z = 0 \tag{18}$$

$$\partial p/\partial x = \mu \frac{\partial^2 V_x}{\partial z^2} \tag{19}$$

$$\partial p/\partial y = \mu \frac{\partial^2 V_y}{\partial z^2} \tag{20}$$

where V_x, V_y, and V_z are the velocity components of flow in the x, y, and z directions, respectively.

The velocity boundary conditions are as follows at different z values:

$$\begin{aligned} &\text{At } z = -h_2, V_x = -V_2,\ V_y = 0,\ V_z = V_2 \frac{\partial h_2}{\partial x} \\ &\text{At } z = h_1, V_x = V_1,\ V_y = 0,\ V_z = V_1 \frac{\partial h_1}{\partial x} \end{aligned} \tag{21}$$

The system above can be reduced to a single equation for the pressure (Reynolds equation):

$$\frac{\partial}{\partial x}\left(h^3 \frac{\partial p}{\partial x}\right) + \frac{\partial}{\partial y}\left(h^3 \frac{\partial p}{\partial y}\right) = 12\mu U \frac{\partial h}{\partial x} \tag{22}$$

where U is the entrainment velocity,

$$U = \frac{V_1 - V_2}{2} \tag{23}$$

Equation 22 would yield negative p in the divergent part of the gap. Because a liquid film cannot sustain negative (gauge) pressure under steady flow

conditions, any negative solution of Eq. 22 would be unrealistic and unacceptable. Hence, the solution domain Ω needs to be determined by the requirement that the pressure is everywhere non-negative, so as to avoid cavitation of the liquid film.

The normal separating force can be obtained by integrating the pressure over the fluid film domain:

$$W = \iint_{\Omega} p\,dx\,dy \tag{24}$$

The friction forces acting on the two surfaces, F_1 and F_2, can be obtained by integrating the shear stresses evaluated on these surfaces:

$$F_{1,2} = \iint_{\Omega} \left[\pm \frac{h}{2}\frac{\partial p}{\partial x} + \frac{\mu(V_1 + V_2)}{h} \right] dx\,dy \tag{25}$$

The volume flow rates entering and leaving the solution domain can be obtained by integrating the unit volume flow rates

$$\begin{aligned} q_x &= \int_{-h_2}^{h_1} V_x\,dz = -\frac{h^3}{12\mu}\frac{\partial p}{\partial x} + Uh \\ q_y &= \int_{-h_2}^{h_1} V_y\,dz = -\frac{h^3}{12\mu}\frac{\partial p}{\partial y} \end{aligned} \tag{26}$$

over appropriate portions of the domain boundary.

It should be noted that, if the two spheres are in relative translation perpendicular to their center line, rather than rotating with respect to each other, there appears to be no entrainment action. However, the analysis is valid in the limiting case of one sphere becoming infinitely large compared with the other, in which case the surface of the large sphere becomes a plane wall and the rotation velocity of the large sphere can be considered as the translation of the plane wall relative to the finite-size sphere (whether in rotation or not). Thus, the result obtained here is applicable to the case of a plane wall sliding past a sphere.

The problem as formulated above has been solved numerically by Dalmaz and Godet[10] and Brewe et al.[11] However, their solutions provide only the pressure distribution and formulas for the normal separating force. For our subsequent analysis, we need not only the normal separating force but also the friction forces and volume flow rate. Because these latter quantities are not available in the literature, the problem needs to be solved more completely.

The problem was discretized by using the finite difference method and solved numerically by using the successive-over-relaxation iterative scheme. The solution domain is determined with Christopherson's algorithm.[12] The integrated properties are obtained by numerical correlation and are given by the following formulas:

Normal separating force

$$W = 9.72411(R_e/h_0)^{0.51953}\ \mu U R_e \tag{27}$$

Friction forces

$$\begin{aligned} F_1 = {} & 2\pi\mu(V_1 + V_2)R_e \ln\left(1 + \frac{1}{2}\frac{R_e}{h_0}\right) \\ & + 3.80525\mu U R_e \ln\left(\frac{R_e}{h_0}\right) - 7.95520\mu U R_e \end{aligned} \tag{28}$$

$$\begin{aligned} F_2 = {} & 2\pi\mu(V_1 + V_2)R_e \ln\left(1 + \frac{1}{2}\frac{R_e}{h_0}\right) \\ & - 3.80525\mu U R_e \ln\left(\frac{R_e}{h_0}\right) + 7.95520\mu U R_e \end{aligned} \tag{29}$$

Volume flow rates

$$Q_{x\_in} = 0.7046 U R_e^2 \tag{30}$$

$$Q_{x\_exit} = 0.3616 U R_e^2 \tag{31}$$

$$Q_y = \pm 0.1715 U R_e^2 \text{ at } y = \pm R_e \tag{32}$$

More details of the solution are given in Yang.[13]

SLUG FLOW MODEL

Consider a dense slurry, containing spherical particles of equal radius R, flowing under a given pressure gradient between two horizontal parallel walls. This paper deals with the simple case that the particles are neutrally buoyant. The particles are kept away from the walls and cluster in the middle of the channel. Therefore, a slug flow model may be envisioned, where the particles are tightly packed together leaving no gap between the closest neighbors, have no relative motion with respect to each other, and move along the channel as a slug. The flow behavior is then solely determined by the interaction between the slug and the walls. From the result of the previous section, this interaction can be characterized by a "tightness parameter" h_0/R, where h_0 is the smallest gap between the particles and the walls.

There are numerous ways in which particles are packed. Three representative packing patterns are studied, viz. rectangular cubic (RC), body-centered cubic (BCC), and face-centered cubic (FCC). Each different packing pattern results in a different volume fraction ϕ. In the case that no gap is left between the closest neighboring particles, the volume fraction takes values of 0.5236 (RC), 0.6802 (BCC), and 0.7405 (FCC), respectively.

Suppose the slug flow can be described by an effective viscosity μ_{eff}; then it is conceivable that the ratio μ_{eff}/μ would be a function of ϕ and h_0/R.

Rectangular Cubic Packing Pattern

One Layer of Spheres ($L \approx 2R$)

This case is shown in Fig. 3a. A train of spheres is translating with velocity V_x down a channel of height L. There is no gap between neighboring spheres, nor is there squeeze action between the spheres and the

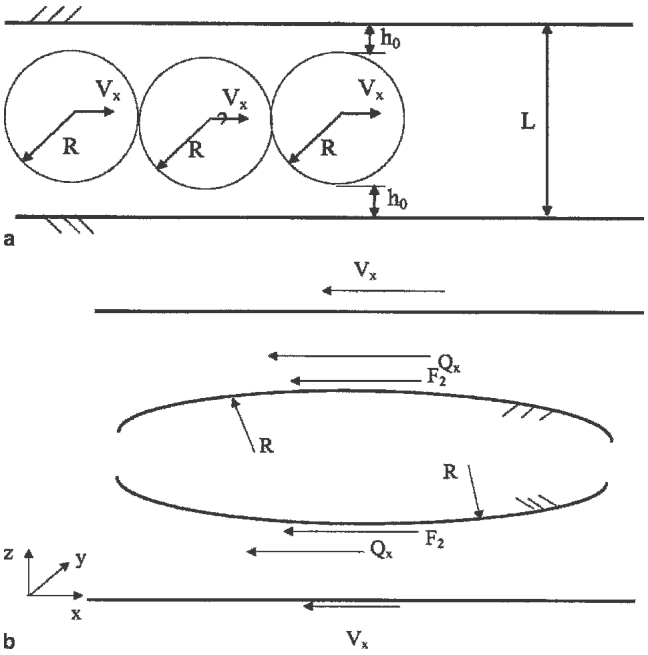

Fig. 3. One layer of spheres translating in a closely spaced channel: (a) flow configuration; (b) entrainment action between a sphere and the walls.

walls. The interaction between one sphere and the walls is detailed in Fig. 3b. The sphere is in equilibrium under the pressure force in the downstream direction and the two friction forces in the upstream direction. The pressure force equals the pressure gradient $(-dp/dx)$ times the volume of the sphere. The friction force F_2 can be obtained from Eq. 29 by setting $V_1 = V_x$, $V_2 = 0$, and $R_e = R$:

$$F_2 \cong 2\pi\mu V_x R\left(\ln\frac{R}{h_0} - \ln 2\right) - 3.80525\mu\frac{V_x}{2}R\ln\frac{R}{h_0} + 7.95520\mu\frac{V_x}{2}R = \mu V_x R[4.38056\ln\frac{R}{h_0} - 0.37757] \equiv \mu V_x R\zeta \tag{33}$$

where the symbol ζ is used to represent the quantity in the square bracket because of the latter's frequent appearance. Thus, the equilibrium equation for the sphere is

$$\left(-\frac{dp}{dx}\right)\frac{4}{3}\pi R^3 = 2\mu V_x R\zeta \tag{34}$$

The volume flow rate (Q) of the slurry down the channel for a channel width 2R (in the y direction) may be written as

$$Q = V_x L2R - 2Q_x \tag{35}$$

where the back flow (Q_x) through the clearance between the sphere and a wall can be obtained from Eq. 31 by setting $U = V_x/2$ and $R_e = R$.

$$Q_x = 0.1808V_x R^2 \tag{36}$$

The slurry flow may be modeled as a plane Poiseuille flow (see Ref. 14, p. 326) with an effective viscosity μ_{eff}:

$$Q = 2R\frac{L^3}{12\mu_{eff}}\left(-\frac{dp}{dx}\right) \tag{37}$$

By substituting Eqs. 34, 35, and 36 into Eq. 37 and rearranging the terms, one obtains a correlation for the effective viscosity:

$$\frac{\mu_{eff}}{\mu} = \frac{1}{8\pi}\left(\frac{L}{R}\right)^3\frac{\zeta}{\left(\frac{L}{R} - 0.1808\right)} \tag{38}$$

Because $L \approx 2R$ in this case, the formula is reduced to

$$\frac{\mu_{eff}}{\mu} = 0.17497\zeta \tag{39}$$

The dependence of the effective viscosity on the tightness parameter is shown in Fig. 4.

n Cells of Rectangular Cubic Packing Pattern ($L \approx ne + 2R$, $e = 2R$, $R_H = 0.60657R$)

Figure 5a shows two layers of spheres in the channel. For the convenience of analysis, let us define the cell size of the rectangular packing to be e × e × e with e = 2R, as shown in the figure. Consider that the channel contains n such cells in the z direction; then, the channel height is approximately

$$L \approx ne + 2R \tag{40}$$

Because the slug is porous, liquid permeates through the pores under the given pressure gradient. To account for the permeated flow, the concept of hydraulic radius[15] is used, which may be defined as two times the ratio of volume to surface of the pore space. The hydraulic radius can be calculated based on one cell, as shown in Fig. 5b.

$$R_H = 2\frac{e^3 - \frac{4}{3}\pi R^3}{4\pi R^2} = 0.60657R \tag{41}$$

Using Poiseuille flow in a capillary (see Ref. 14, p. 337) to model the permeated flow, the volume flow rate for one cell is

$$Q_p = \frac{\pi R_H^4}{8\mu}\left(-\frac{dp}{dx}\right) \tag{42}$$

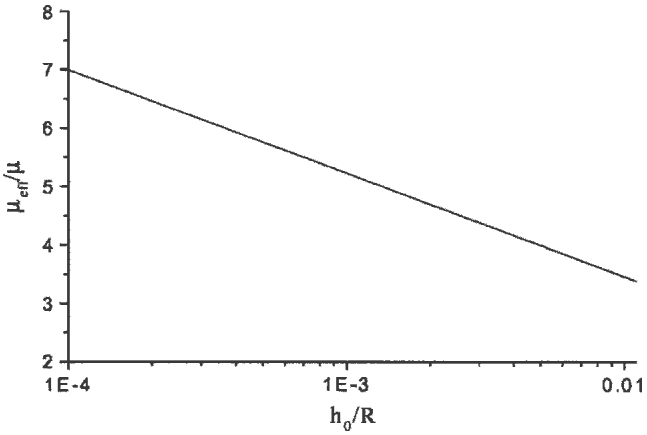

Fig. 4. Effective viscosity as a function of h_0/R (one layer of spheres in the channel).

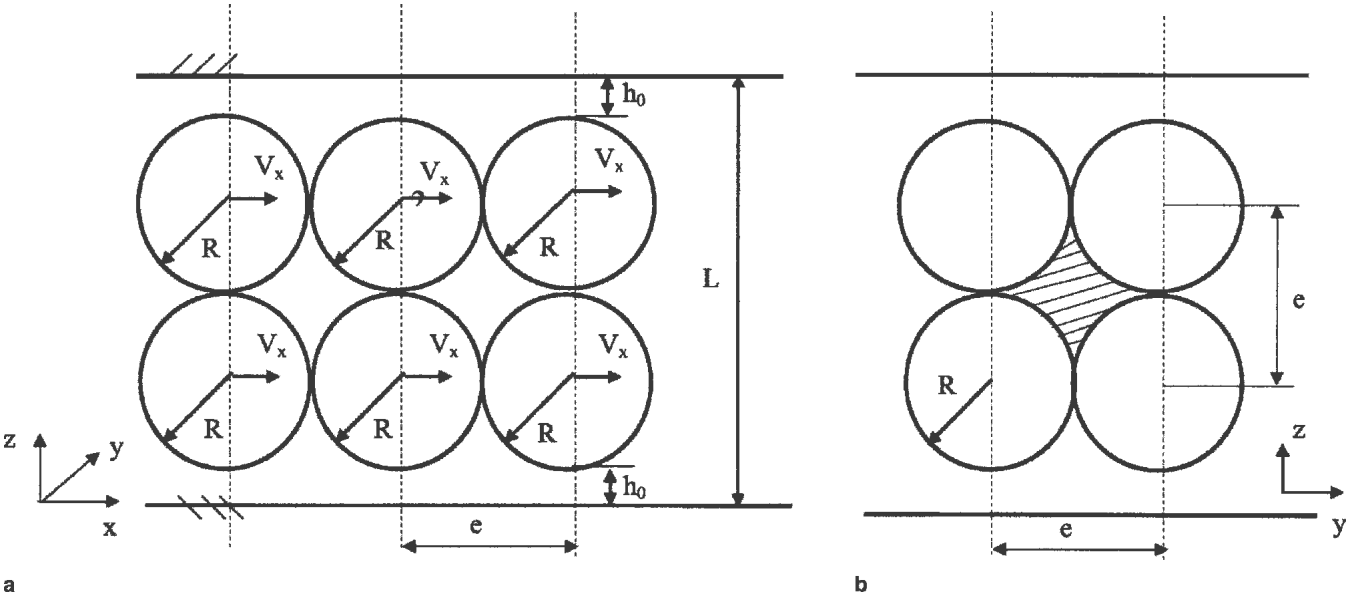

Fig. 5. RC packing (two layers): (a) as viewed in the (x,z) plane; (b) as viewed in the (y,z) plane (lightly drawn lines show the leakage path).

and the friction force exerted by the permeated flow in one cell on the slug (acting in the downstream direction) is

$$F_p = \pi R_H^2 \left(-\frac{dp}{dx}\right) e \tag{43}$$

The equilibrium equation for a slug of dimensions $e \times e$ in the (x, y) plane but consisting of n cells in the z direction is

$$\left(-\frac{dp}{dx}\right)(n+1)\frac{4}{3}\pi R^3 + nF_p = 2F_2 \tag{44}$$

The volume flow rate of the slurry for a channel width e is

$$Q = V_x Le + nQ_p - 2Q_x \tag{45}$$

Note that F_2 and Q_x remain to be given by Eqs. 33 and 36. Again, using the plane Poiseuille flow formula

$$Q = e\frac{L^3}{12\mu_{eff}}\left(-\frac{dp}{dx}\right) \tag{46}$$

to correlate the result, we obtain

$$\frac{\mu_{eff}}{\mu} = \frac{1}{6\pi}\left(\frac{L}{R}\right)^3 \frac{\zeta}{\left[\frac{L}{R} - 2(0.1808)\frac{R}{e}\right]\left[\frac{4}{3}(n+1) + n\left(\frac{R_H}{R}\right)^2\frac{e}{R}\right] + \frac{n}{4}\left(\frac{R_H}{R}\right)^4\left(\frac{R}{e}\right)\zeta} \tag{47}$$

Note that in this case $L \approx (n+1)2R$, $e = 2R$, and R_H is given by Eq. 41. According to Eq. 47, the effective viscosity increases with n. The solid and dashed lines in Fig. 6 show the dependence of the effective viscosity on the number of cells and the tightness parameter.

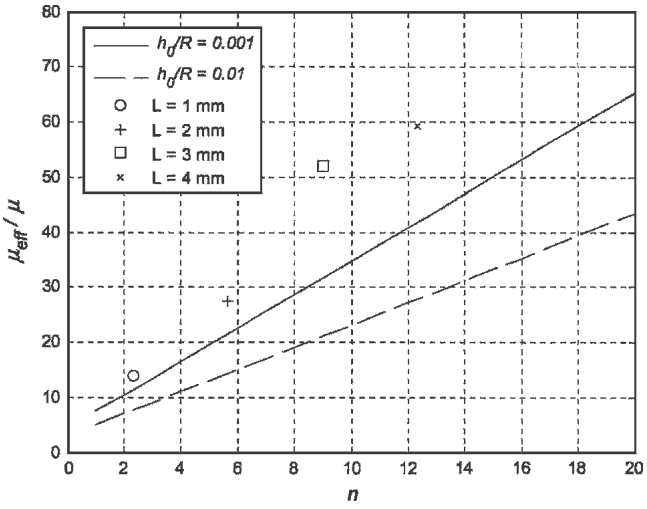

Fig. 6. Effective viscosity in RC packing.

Body-Centered Cubic Packing Pattern ($L \approx ne + 2R$, $e = 2.30940R$, and $R_H = 0.31347R$)

In the BCC packing pattern there are eight spheres at the vertices of a cube and one sphere at the center of the cube. Figure 7a shows one cell of this pattern. When the spheres are packed so closely that there is no gap between the center sphere and the corner spheres, the cell size is given by

$$e = \frac{4}{\sqrt{3}}R = 2.30940R \tag{48}$$

Consider that the channel contains n body-centered cells in the z direction. Figure 7b shows this case for $n = 1$. The channel height is then approximately

$$L \approx ne + 2R \tag{49}$$

The hydraulic radius can be calculated, based on one cell, as

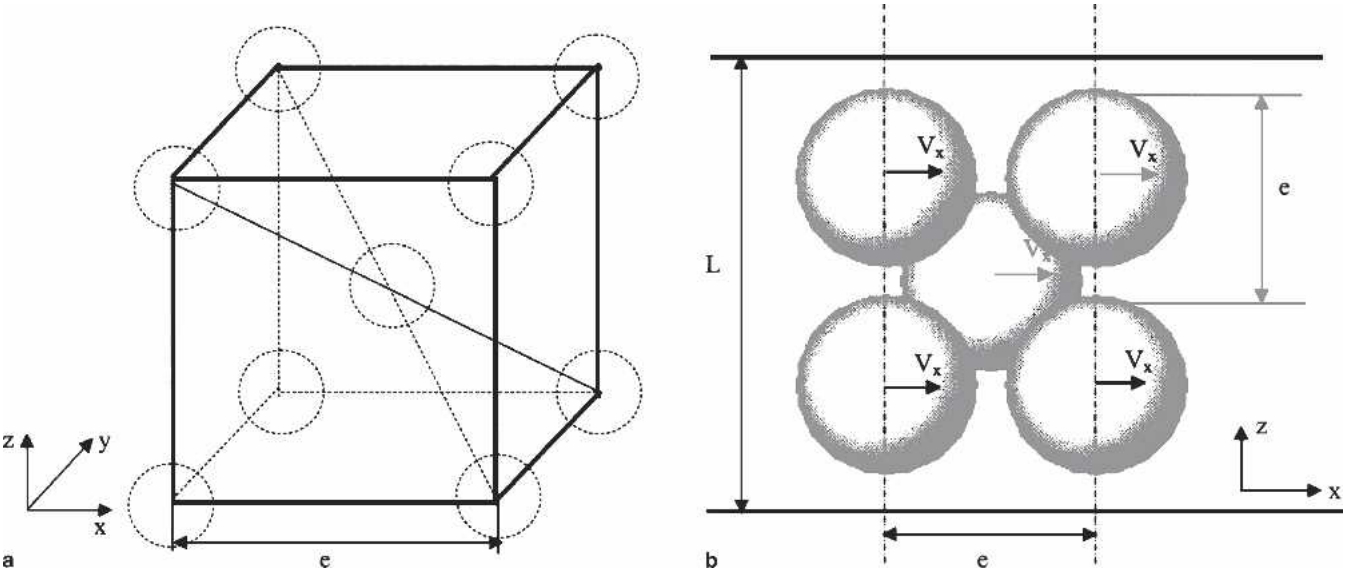

Fig. 7. BCC packing: (a) location of spheres; (b) one cell in the channel.

$$R_H = 2\frac{e^3 - 2\left(\frac{4}{3}\pi R^3\right)}{2(4\pi R^2)} = 0.31347R \qquad (50)$$

The equilibrium equation for a slug of dimension e × e in the (x, y) plane but consisting of n cells in the z direction is

$$\left(-\frac{dp}{dx}\right)(2n+1)\frac{4}{3}\pi R^3 + nF_p = 2F_2 \qquad (51)$$

The volume flow rate of the slurry for a channel width e is given by Eq. 45. Following the same procedure as was done in the section "n Cells of Rectangular Cubic Packing Pattern," we obtain

$$\frac{\mu_{eff}}{\mu} = \frac{1}{6\pi}\left(\frac{L}{R}\right)^3 \frac{\zeta}{\left[\frac{L}{R} - 2(0.1808)\frac{R}{e}\right]\left[\frac{4}{3}(2n+1) + n\left(\frac{R_H}{R}\right)^2\frac{e}{R}\right] + \frac{n}{4}\left(\frac{R_H}{R}\right)^4\frac{R}{e}\zeta} \qquad (52)$$

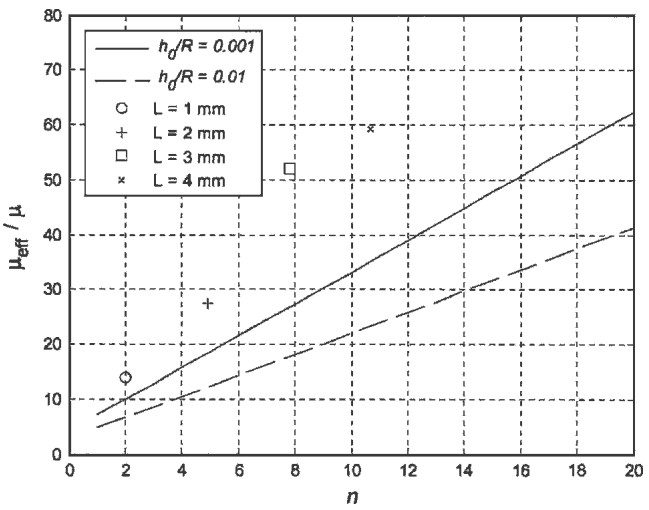

Fig. 8. Effective viscosity in BCC packing.

Equation 52 differs from Eq. 47 only slightly. However, in this case e and R_H are given by Eqs. 48 and 50, respectively. The solid and dashed lines in Fig. 8 show the effective viscosity as a function of n and h_0/R.

Face-Centered Cubic Packing Pattern ($L \approx ne + 2R$, $e = 2.82843R$, $R_H = 0.23366R$)

In the FCC packing pattern there are eight spheres at the vertices of a cube and a sphere at the center of each of the six faces. Figure 9a shows one cell of this pattern. When the spheres are packed so closely that there is no gap between the center sphere and the corner spheres on any face, the cell size is given by

$$e = 2\sqrt{2}R = 2.82843R \qquad (53)$$

Consider that the channel contains n such cells in the z direction. Figure 9b shows this case for n = 1. The channel height is (approximately) still given by $L \approx ne + 2R$. The hydraulic radius can be calculated, based on one cell, as

$$R_H = 2\frac{e^3 - 4\left(\frac{4}{3}\pi R^3\right)}{4(4\pi R^2)} = 0.23366R \qquad (54)$$

The equilibrium equation for a slug of dimension e × e in the (x, y) plane but consisting of n cells in the z direction is

$$\left(-\frac{dp}{dx}\right)(4n+2)\frac{4}{3}\pi R^3 + nF_p = 4F_2 \qquad (55)$$

The volume flow rate of the slurry for a channel width e is

$$Q = V_x Le + nQ_p - 4Q_x \qquad (56)$$

Following the same procedure as was done in the section "n Cells of Rectangular Cubic Packing Pattern," we obtain

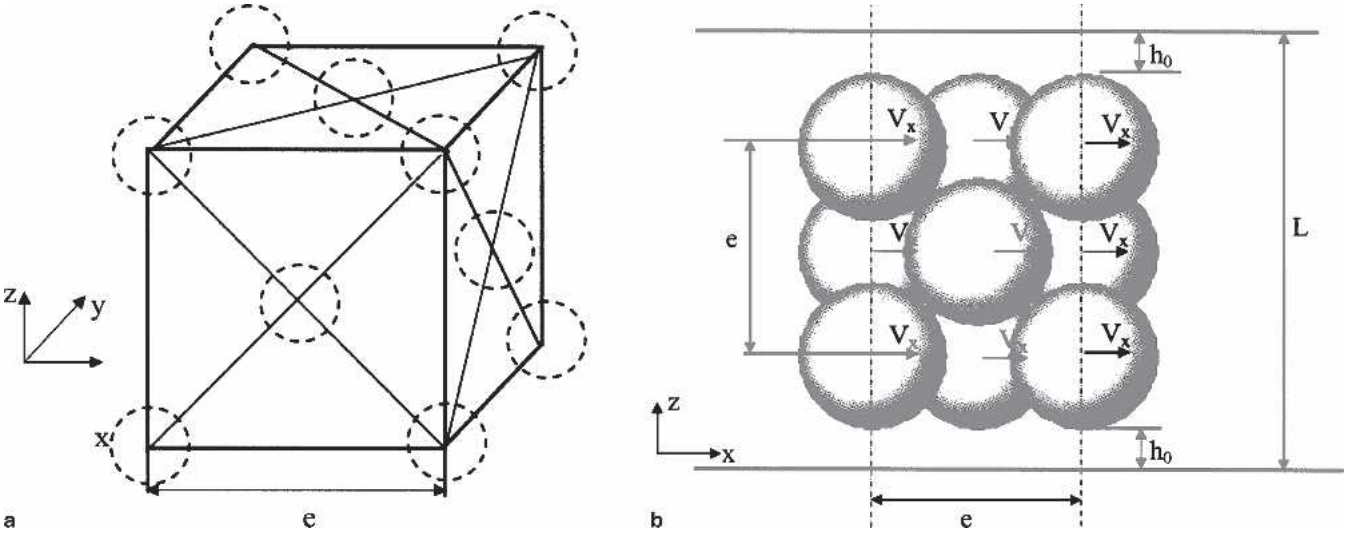

Fig. 9. FCC packing: (a) location of spheres; (b) one cell in the channel.

$$\frac{\mu_{\text{eff}}}{\mu} = \frac{1}{3\pi}\left(\frac{L}{R}\right)^3 \frac{\zeta}{\left[\frac{L}{R} - 4(0.1808)\frac{R}{e}\right]\left[\frac{4}{3}(4n+2) + n\left(\frac{R_H}{R}\right)^2\frac{e}{R}\right] + \frac{n}{2}\left(\frac{R_H}{R}\right)^4\frac{R}{e}\zeta} \tag{57}$$

In this case, e and R_H are given by Eqs. 53 and 54. The solid and dashed lines in Fig. 10 show the effective viscosity as a function of n and h_0/R.

SUMMARY AND DISCUSSION

This work was motivated by the need to model the underfill encapsulant flows, which are slurries consisting of liquid carriers and filling particles in high volume fraction. It is postulated that the flow behavior of such dense slurries is governed by the particle-particle and particle-wall interactions. These interactions are realized through thin liquid films trapped between the solid surfaces. In the section "Unit Solutions for Interactions Between Two Particles," fluid film lubrication theory was used to obtain the formulas for these interactions, including the normal separating force and friction forces acting on the surfaces and the film flow rate between the surfaces. These formulas are new and readily usable for evaluating the effects of fluid film lubrication.

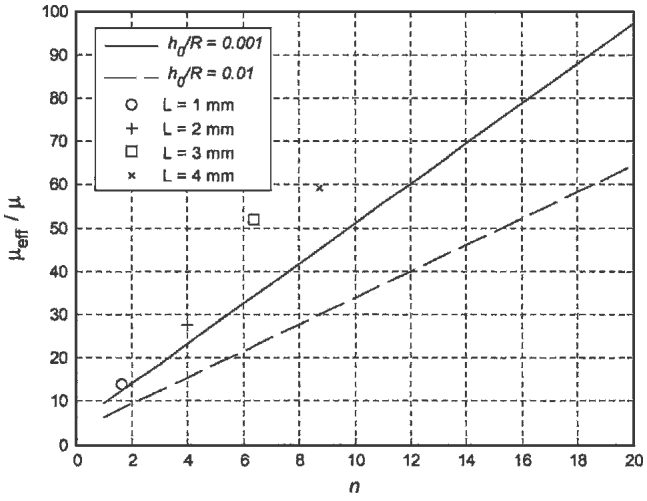

Fig. 10. Effective viscosity in FCC packing.

In the section "Slug Flow Model," these lubrication formulas were applied to the slug flow of a dense slurry, under a pressure gradient, between two parallel walls. Three closed-form formulas for the effective viscosity, Eqs. 47, 52, and 57, were obtained for the RC, BCC, and FCC packing patterns, respectively. The volume fraction values of these patterns are 0.5236, 0.6802, and 0.7405, respectively. These formulas reveal the dependence of the effective viscosity on the packing pattern, the tightness parameter h_0/R, and the number of cells n contained in the channel height. Contrary to the predictions by other viscosity formulas in the literature, the current model shows that the effective viscosity is finite in the high volume fraction limit.

Several limitations of the proposed theory should be noted. Because lubrication theory is used, the packing of solid particles should be near the dense limit or the tightness parameter should be small. One should expect the theory to break down if the tightness parameter becomes >0.01. Within the validity of lubrication theory, it is clear that a smaller h_0/R results in a large wall drag and hence a higher μ_{eff}/μ.

The filling particles in slurry probably would not flow in a prescribed formation, yet only three specific packing patterns were considered. Despite our ignorance of the flow formation, it may be reasoned that different packing patterns in essence expose different numbers of interaction points between the slug and the walls and provide different degrees of permeability of the porous slug. However, results of the current study (Figs. 6, 8, and 10) show that

the three patterns yield qualitatively the same picture. It may thus be conjectured that the true formation would yield this same qualitative picture.

Lubrication effects are stronger with a smaller tightness parameter. When a sphere interacts with another sphere, the reduced radius given by Eq. 4 is R/2. When a sphere interacts with a plane wall, the reduced radius is R. The latter produces a smaller tightness parameter for the same h_0. Hence, the particle-wall interaction is stronger than the particle-particle interaction. As a result, the particles are kept away from the walls and cluster in the middle of the channel. A slug flow model was therefore adopted to model the slurry flow. The simple experiment mentioned in the Introduction also provided justification for adopting this model. The model, however, produces a pronounced effect of n on μ_{eff}. Note that the volume flow rate of a slug flow is basically proportional to the channel height L (which is essentially proportional to n), whereas that of the plane Poiseuille flow is proportional to L^3. If the former is to be correlated by the latter, the effective viscosity must increase with L^2 (or proportional to n^2). On the other hand, for the same pressure gradient, a large L causes a proportional increase in the pressure force on the slug while the wall drag remains the same, which causes the flow rate to increase, or equivalently, the effective viscosity to decrease. Competition between these two factors results in an almost linear increase of μ_{eff} with n. This result is a consequence of the slug flow model. One might conceive that, as the channel height becomes large, departure from slug flow behavior would become more likely. The question of how large n can be for the slug flow model to remain usable should be answered by experiment.

In addition, the proposed theory considers only the situation of one size, neutrally buoyant, spherical particles. If the distribution of particle size is bimodal or broadly dispersed, the packing of particles would be denser and its porosity smaller, resulting in a smaller permeated flow through the slug. Meanwhile, interaction of the slug with the channel walls would still be dominated by the large particles. The combined effect of these factors on the effective viscosity requires further investigation. The case of non-spherical particles can perhaps be treated with an appropriate shape factor. The effect of non-neutrally buoyant particles is addressed in a separate paper.[16]

EXPERIMENTAL VERIFICATION

An experiment aimed at comparing the proposed theory with measurements was conducted. Several flow channels of rectangular cross section and different channel heights (1–4 mm) were made by gluing glass slides (25 × 53 mm) together. Side clearances of the flow channels were sealed. Upstream of each flow channel was a storage tank, also made of glass slides, where a constant head (typically 60 mm of the slurry) was maintained. Flow rates were determined by measuring the weight of the collected flow at the downstream end of the channel (which was at the ambient condition) during a given time interval (typically 5–15 min.). The effective viscosity of the slurry was calculated by using the plane Poiseuille flow formula. A schematic diagram of the flow channel is shown in Fig. 11.

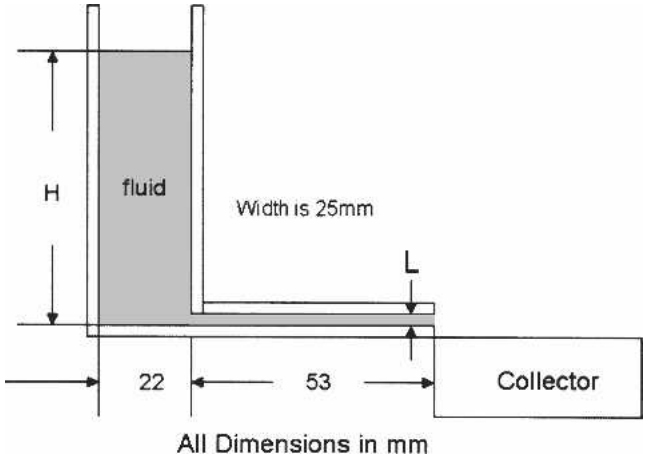

Fig. 11. Schematic diagram of the experimental flow channel.

Two kinds of slurries were prepared: one by mixing PMMA particles (of density 1190 kg/m^3 and diameter 200–400 μm) with glycerine (of density 1261 kg/m^3 and viscosity 1.41 Pa s), the other by mixing glass beads (of density 2550 kg/m^3 and diameter 200 μm) with honey (of density 1340–1400 kg/m^3 and viscosity 5.07 Pa s). The former was used to approximate the situation of neutrally buoyant particles, and the latter to investigate the effect of heavier filler particles. The measured results of using PMMA particles with glycerine are plotted in Figs. 6, 8, and 10 along with theoretical predictions. Each data point represents the result of five repeated measurements. These data points were obtained with a carefully controlled $\phi = 0.55$.

The results clearly display the slug flow characteristics, viz. the effective viscosity increases with the number of cells contained in the channel height. In addition, the data points lie closer to the theoretical prediction of a smaller tightness parameter, indicating that lubrication mechanisms correctly describe the interaction between the slug and channel walls. Appreciable quantitative differences between the theoretical predictions and measurements remain. However, in view of the simplicity of the theory, and the crude approximations made therein, such deviations might be considered reasonable. The experiment was carried only up to a channel height of 4 mm due to expense.

ACKNOWLEDGEMENTS

This research was partially supported by the U.S. Navy Naval Surface Warfare Center under Grant 240-6568A. The research was also funded by the Integrated Electronics Engineering Center at the State University of New York at Binghamton. The IEEC receives funding from the New York State Science

and Technology Foundation, the National Science Foundation, and a consortium of industrial members.

REFERENCES

1. E.W. Washburn, *Phys. Rev.* 17, 273 (1921).
2. S. Han, K.K. Wang, and S.-Y. Cho, *Electronic Components and Technology Conference*(Orlando, FL: 1996), pp. 327–334.
3. L.T. Nguyen, A.S. Chen, A. Krishnan, S.A. Bayyuk, S.A. Lowry, A.J. Przekwas, and S.A. Bidstrup-Allen, InterPack 97, Hawaii, June 1997, pp. 15–19.
4. A. Einstein, *Ann. Phys.* 19, 289 (1906).
5. D. Leighton and A. Acrivos, *Chem. Eng. Sci.* 41, 1377 (1986).
6. H.H. Hu, *Int. J. Multiphase Flow* 22, 335 (1996).
7. D. Prasad and H.K. Kytomaa, *Int. J. Multiphase Flow* 21, 775 (1995).
8. Y. Guo, G.L. Lehmann, T. Driscoll, and E.J. Cotts, *1999 Electronic Components and Technology Conference* (1999), pp. 71–76.
9. A. Acrivos, *Particulate Two-Phase Flow*, ed. M.C. Rico (New York: Butterworth-Heinemann, 1993), Chap. 5, pp. 169–189.
10. G. Dalmaz and M. Godet, *J. Mech. Eng. Sci.* 15, 400 (1973).
11. D.E. Brewe, B.J. Hamrock, and C.M. Taylor, *J. Lubr. Technol.* 101, 231 (1979).
12. D.G. Christopherson, *Proc. Inst. Mech. Eng.* 146, 126 (1941).
13. R. Yang, M.S. thesis, State University of New York at Binghamton, NY (1998).
14. R.W. Fox and A.T. McDonald, *Introduction to Fluid Mechanics*, 4th ed. (New York: Wiley, 1992).
15. A.E. Scheidegger, *The Physics of Flow Through Porous Media* (Toronto: University of Toronto Press, 1963), p. 124.
16. R. Yang, D.C. Sun, and S. Park, *J. Electron. Mater* 35, 2026 (2006).

SYMBOLS

e	cell size
F_1, F_2	friction forces
F_p	friction force exerted by permeated flow on a slug cell
h_0	smallest gap between two interacting surfaces
L	channel height
n	number of cells contained in channel height
p	pressure
Q	volume flow rate
Q_p	permeated flow rate through a slug cell
R	particle radius
R_e	reduced radius, defined in Eq. (4)
R_H	hydraulic radius
U	entrainment velocity, defined in Eq. (23)
V_1, V_2	velocities of interacting surfaces
W	normal separating force
(x, y, z)	coordinate system
ζ	a quantity defined in Eq. (33)
μ	viscosity of liquid carrier
μ_{eff}	effective viscosity of slurry
ϕ	volume fraction
ϕ_0	volume fraction at the closest packing